What Determines the Redox Potential of Ferredoxins?

T. Essigke[a], G.M. Ullmann[b], R.C. Wade[a]

[a]European Media Laboratory, Schloss-Wolfsbrunnenweg 33,
69118 Heidelberg, Germany
[b]Institute of Scientific Computing, University of Heidelberg, Im Neuenheimer Feld 368,
69120 Heidelberg, Germany

Summary:
For many cytochromes P450 (P450), the electrons are transferred from the reductase to the P450 via a [2Fe-2S] cluster ferredoxin (e.g. putidaredoxin, terpredoxin or adrenodoxin). A similar role is played by several plant-type ferredoxins to transfer electrons from photosystem I to $NADP^+$. Other ferredoxins like *E. coli* ferredoxin are probably involved in the biogenesis of iron-sulfur clusters. To understand what modulates the redox potential of the metal center in the different proteins, we have developed a method to calculate redox potentials from first principles. In calculations for *Anabaena PCC7119* ferredoxin, we found that certain changes in protein structure upon a change in redox state have a strong influence on the redox potential. Preliminary results indicate that the same mechanism may be important for determining the redox potentials of other ferredoxins.

Introduction:

The small iron-sulfur proteins of the [2Fe-2S] cluster ferredoxin family have been under intensive investigation in recent years because of their importance in electron transfer reactions, such as those in the P450 system and in photosynthesis. Some of these iron-sulfur cluster proteins are very well characterized biochemically (Grinberg et al 2000) and structurally by crystallography and NMR (see references below). Nevertheless, it is still unclear how the redox potential is modulated by the protein. The effect of mutants cannot be predicted and the results from experiments are often counter-intuitive (Zöllner et al. 2002).

Considering the P450 system, NMR structures have been determined for putidaredoxin and terpredoxin but these do not give an accurate picture of the region around the iron-sulfur cluster because of line broadening at the iron-sulfur center or the replacement of Fe^{3+} by Ga^{3+} for structure determination (Kostic et al. 2002). The crystal structures of adrenodoxin show residues 4-108 (Müller et al. 1998) or 6-111 (Pikuleva

et al. 2000) of the 128 residues in the oxidized state, but the structure of the C-terminal part is unknown. It is most likely unstructured in the oxidized state, but might adapt a more rigid conformation in the reduced state. Whether adrenodoxin acts as a monomer or dimer is under debate (Beilke et al. 2002).

The structural data are much clearer for plant-type ferredoxins involved in photosynthesis. There are high-resolution crystal structures of *Anabaena* ferredoxin in both the oxidized and reduced states (Morales et al. 1999) (see Figure 1) and there are also structures of several mutants available (Hurley et al. 1997). Consequently, we have first applied our methodology to compute redox potentials to *Anabaena* ferredoxin and then applied it to ferredoxins in the P450 system.

In the following sections, we give a brief outline of the method used, present results of calculations on *Anabaena* and *E. coli* ferredoxins and on adrenodoxin, and finally discuss the effects modulating the redox potential and their potential importance in [2Fe-2S] cluster ferredoxins.

Methods:

Our approach is to combine a density function theory quantum mechanical treatment of the iron-sulfur cluster with a classical electrostatics treatment of the surrounding protein environment. The protocol is similar to that published earlier (see Ullmann et al. 2002 and references therein; Li et al. 1998).

The quantum mechanics calculation is used to obtain the difference in the energy of the iron-sulfur center in the two redox states in vacuum ($\Delta H^{ox\rightarrow red}_{vac}$). It also provides the electrostatic potential to which point charges at the coordinates of the atoms of the iron-sulfur cluster are fitted. The fitted atomic partial charges for the metal center and standard force field atomic charges for the protein are used in Poisson-Boltzmann electrostatics calculations to compute the difference in the solvation energy ($\Delta\Delta G^{ox\rightarrow red}_{solv}$) of the metal center in the protein and water in the two redox states.

The redox potential (E^{redox}) is then calculated using a thermodynamic cycle (see Figure 2):

$$E^{redox} = - (\Delta H^{ox\rightarrow red}_{vac} + \Delta\Delta G^{ox\rightarrow red}_{solv})/F + \Delta SHE$$

Here, F is the Faraday constant (23.06 kcal/(mol V)) and ΔSHE is the standard potential of the hydrogen electrode (-4.43 V).

Results:

The redox potential measured for *Anabaena* ferredoxin varies over a range of about 60 meV (see Table 1), and depends on the method used by different authors (see discussion in Hurley et al. 1997). The redox potentials calculated previously differ by over 100 meV from the closest experimental value.

We calculated the redox potential either using a single protein conformation or including treatment of conformational changes present in the different crystal structures of *Anabaena* ferredoxin and in the modeled hydrogen atom positions. When taking only a single conformation into account, we failed to reproduce the experimental results by over 500 meV, although we reproduced very well the results of Li et al., 1998 (who based their calculations on a single structure). On the other hand, when the change in protein conformation on redox state change is accounted for in the calculations, we obtained much better agreement with experiment.

For *E. coli* ferredoxin and adrenodoxin (residues 4-108), crystal structures are only available for the oxidized state. Our calculation without treating conformational change has about the same difference compared to experiment as the respective calculation for *Anabaena* ferredoxin. Therefore, we expect that adrenodoxin also undergoes conformational changes upon reduction, which might be similar to those in *Anabaena* ferredoxin as the energetic contribution to the redox potential is about the same.

Conclusions:

Our combined quantum mechanics/continuum electrostatics method provides a promising approach to compute the redox potentials of ferredoxins from first principles. The results show that it is necessary to account for conformational changes upon a change in redox state in order to obtain results in agreement with experiments. However, the modeling work necessary also leads to larger uncertainties in the calculated redox potential values.

The order of magnitude of the contribution to the redox potential due to conformational change seems to be the same for the studied ferredoxin and adrenodoxin proteins. Further investigations will show whether there is a common mechanism for modulating their redox potential by conformational changes.

Acknowledgments:

TE and RCW thank the Klaus Tschira Foundation and GMU thanks the DFG for financial support. We are grateful for helpful discussions with

Prof. R. Bernhardt and her group (University of Saarbrücken). We are also thankful for computer time provided by Prof. Lindenstruth at the Kirchhoff Institute of Physics (University of Heidelberg) and by the Helics-Team at the Institute of Scientific Computing (University of Heidelberg).

References:

D. Beilke, R. Weiss , F. Löhr , P. Pristovsek , F. Hannemann , R. Bernhardt , H. Rüterjans, A new electron transport mechanism in mitochondrial steroid hydroxylase systems based on structural changes upon the reduction of adrenodoxin, Biochemistry, 41, 7969-7978, 2002.

A. V. Grinberg , F. Hannemann , B. Schiffler , J. Müller , U. Heinemann , R. Bernhardt, Adrenodoxin: structure, stability, and electron transfer properties, Proteins 40, 590-612, 2000.

J. K. Hurley , Z. Salamon , T. E. Meyer , J. C. Fitch , M. A. Cusanovich , J. L. Markley , H. Cheng , B. Xia , Y. K. Chae , M. Medina , C. Gomez-Moreno , G. Tollin, Amino acid residues in Anabaena ferredoxin crucial to interaction with ferredoxin-NADP+ reductase: site-directed mutagenesis and laser flash photolysis, Biochemistry 32, 9346-9354, 1993.

J. K. Hurley , A. M. Weber-Main , M. T. Stankovich , M. M. Benning , J. B. Thoden , J. L. Vanhooke , H. M. Holden , Y. K. Chae , B. Xia , H. Cheng , J. L. Markley , M. Martinez-Julvez , C. Gomez-Moreno , J. L. Schmeits , G. Tollin. Structure-function relationships in Anabaena ferredoxin: correlations between X-ray crystal structures, reduction potentials, and rate constants of electron transfer to ferredoxin:NADP+ reductase for site-specific ferredoxin mutants, Biochemistry 36, 11100-11117, 1997.

Y. Kakuta, T. Horio, Y. Takahashi, K. Fukuyama, Crystal Structure of Escherichia coli Fdx, an Adrenodoxin-Type Ferredoxin Involved in the Assembly of Iron-Sulfur Clusters, Biochemistry 40, 11007-11012, 2001.

M. Kostic, S. S. Pochapsky, J. Obenauer, H. Mo, G.M. Pagani, R. Pejchal, T.C. Pochapsky, Comparison of functional domains in vertebrate-type ferredoxins. Biochemistry 41, 5978-5989, 2002.

J. Li, M.R. Nelson, Ch. Y. Peng, D. Bashford , L. Noodleman, Incorporating Protein Environments in Density Functional Theory: A Self-Consistent Reaction Field Calculation of Redox Potentials of [2Fe2S]

Clusters in Ferredoxin and Phthalate Dioxygenase Reductase, J. Phys. Chem. A 102, 6311 -6324, 1998.

R. Morales , M. H. Charon , G. Hudry-Clergeon , Y. Petillot , S. Norager , M. Medina , M. Frey, Refined X-ray structures of the oxidized, at 1.3 A, and reduced, at 1.17 A, [2Fe-2S] ferredoxin from the cyanobacterium Anabaena PCC7119 show redox-linked conformational changes, Biochemistry 38, 15764-15773, 1999.

A. Müller , J. J. Müller , Y. A. Müller , H. Uhlmann , R. Bernhardt , U. Heinemann, New aspects of electron transfer revealed by the crystal structure of a truncated bovine adrenodoxin, Adx(4-108), Structure 6, 269-280, 1998.

P. J. Stephens , D. R. Jollie , A. Warshel, Protein Control of Redox Potentials of Iron-Sulfur Proteins, Chem. Rev. 96, 2491-2514, 1996.

I. A. Pikuleva , K. Tesh , M. R. Waterman , Y. Kim, The tertiary structure of full-length bovine adrenodoxin suggests functional dimers, Arch. Biochem. Biophys. 373, 44-55, 2000

H. Uhlmann , S. Iametti , G. Vecchio , F. Bonomi , R. Bernhardt, Pro108 is important for folding and stabilization of adrenal ferredoxin, but does not influence the functional properties of the protein, Eur. J. Biochem. 248, 897-902, 1997.

H. Uhlmann, Die Rolle von Threonin-54, Cystein-Resten sowie der N- und C-terminalen Bereiche des adrenalen Ferredoxins, PhD Thesis Humboldt Universität, Berlin 1995.

G. M. Ullmann , L. Noodleman , D. A. Case, Density functional calculation of p K(a) values and redox potentials in the bovine Rieske iron-sulfur protein, J. Biol. Inorg. Chem. 7, 632-639, 2002

A. Zöllner, F. Hannemann, M. Lisurek, R. Bernhardt, Deletions in the loop surrounding the iron sulfur cluster of adrenodoxin severely affect the interactions with its native redox partners adrenodoxin reductase and cytochrome P450scc (CYP11A1), J. Inorg. Biochem. 91, 644-654, 2002.

Figure Captions:

Figure 1. Structure of *Anabaena* ferredoxin showing the location of secondary structure elements and the iron-sulfur cluster (Fe: green; S: yellow).

Figure 2. Scheme showing thermodynamic cycle used to compute the redox potential (see text).

Table 1. Experimental and calculated Redox Potentials

Method	E^{redox} [meV]	Reference
Anabaena PCC7119 Ferredoxin		
Experiment	-440 ± 15	Hurley et al. 1993
Experiment	-382 ± 1-3	Hurley et al. 1997
Calculated	-955	Li et al. 1998
Calculated	-267	Stephens et al. 1996
Calculated	-653	Stephens et al. 1996
Calculated (without conformational change)	-957 ± 13	Present work
Calculated (with conformational change)	-450±120	Present work
E. coli Ferredoxin		
Experiment	-380	Kakuta et al. 2001
Calculated (without conformational change)	-931 ± 27	Present work
Bovine Adrenodoxin		
Experiment (wild-type)	-273	Uhlmann 1995
Experiment (residues 4-108)	-344	Uhlmann et al. 1997
Calculated (residues 4-108) (without conformational change)	-886 ± 20	Present work

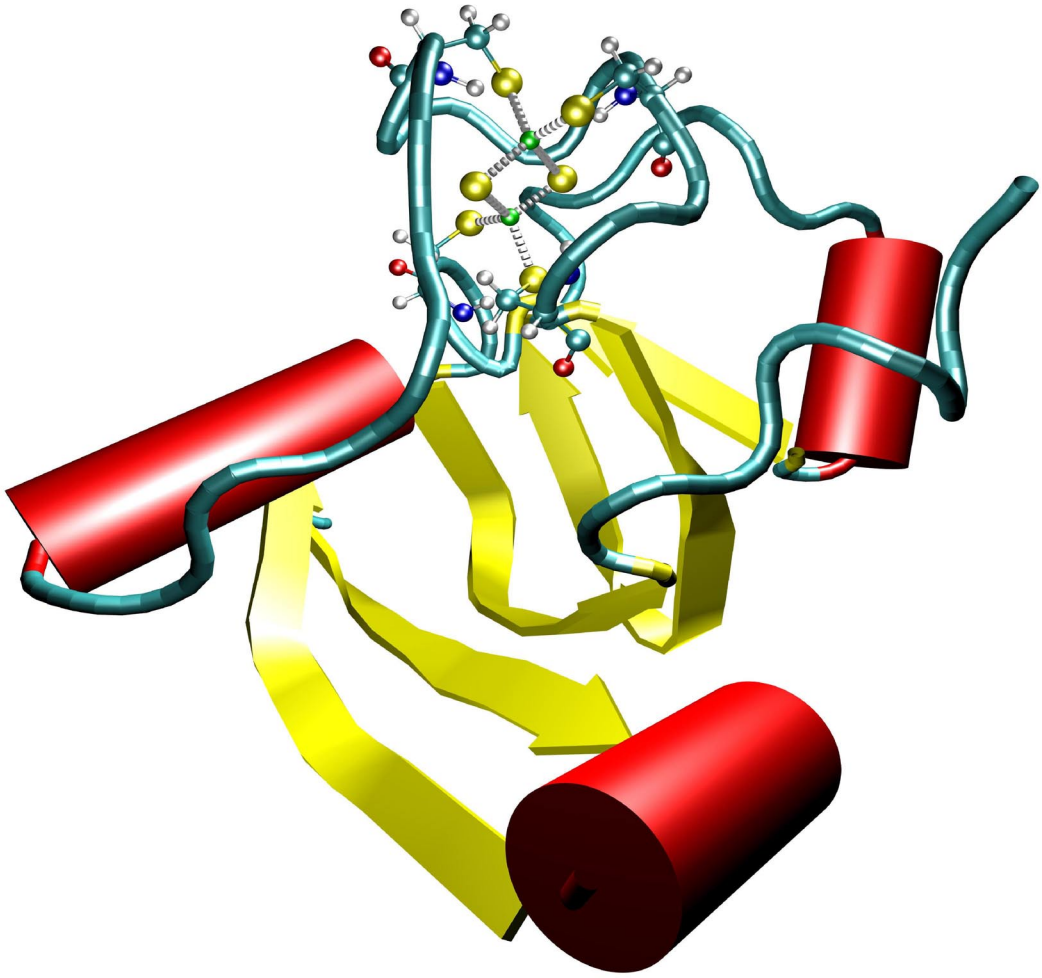

Figure 1. Structure of *Anabaena* ferredoxin showing the location of secondary structure elements and the iron-sulfur cluster (Fe: green; S: yellow).

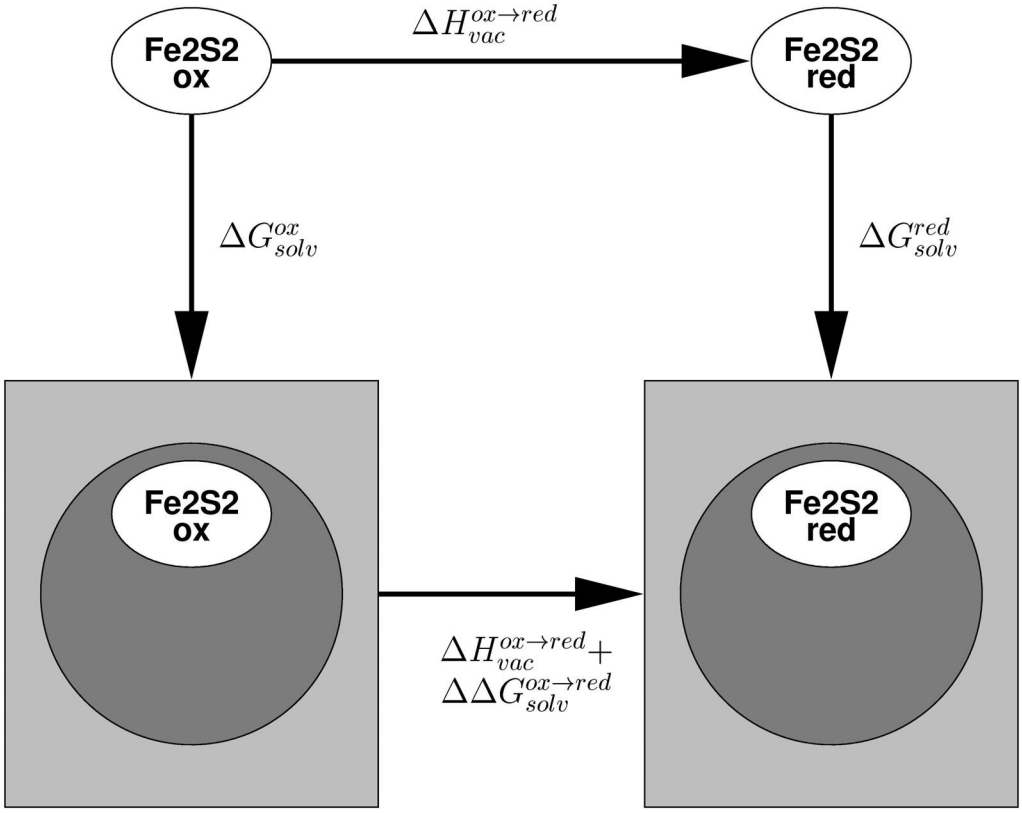

Figure 2. Scheme showing thermodynamic cycle used to compute the redox potential (see text).